Lifetimes of high-spin states in the $\pi i_{13/2}$ band of ^{173}Re

N. R. Johnson,[1,2] J. C. Wells,[1,3] Y. Akovali,[1] C. Baktash,[1] R. Bengtsson,[4] M. J. Brinkman,[1] D. M. Cullen,[1,*] C. J. Gross,[1,5] H.-Q. Jin,[1] I.-Y. Lee,[6] A. O. Macchiavelli,[6] F. K. McGowan,[1] W. T. Milner,[1] and C.-H. Yu[1,7]

[1]*Oak Ridge National Laboratory, Oak Ridge, Tennessee 37831*

[2]*Joint Institute for Heavy Ion Research, Oak Ridge, Tennessee 37831*

[3]*Tennessee Technological University, Cookeville, Tennessee 38505*

[4]*Lund Institute of Technology, Lund, Sweden*

[5]*ORISE, Oak Ridge Associated Universities, Oak Ridge, Tennessee 37830*

[6]*Lawrence Berkeley National Laboratory, Berkeley, California 94720*

[7]*University of Rochester, Rochester, New York 14627*

(Received 30 September 1996)

Lifetime measurements on the $i_{13/2}$ band built on the proton configuration $1/2^+[660]$ in ^{173}Re have been carried out by the Doppler-broadened line shape method with the use of the GAMMASPHERE array in an early-implementation arrangement. Lifetimes of the stretched $E2$ transitions from states of spin $41/2^+ - 69/2^+$ in this band were measured, and the transition quadrupole moments calculated from these lifetimes are consistent (average $Q_t = 8.1 \pm 0.5$ e b) with a large and near-constant deformation ($\beta_2 \approx 0.29$) over the frequency range of $\hbar\omega = 0.29 - 0.47$ MeV. This result attests to the strong deformation-driving effect of the intruder $\pi i_{13/2}$ orbital when it lies just above the Fermi surface. From thin-target measurements, it was possible to add three new levels to this band and to determine that the experimental aligned angular momenta gradually evolve over a large frequency range and level off with a total gain characteristic of alignment by $i_{13/2}$ neutrons. Calculations carried out for diabatic configurations give a satisfactory accounting of the alignment gain. However, because of the large interaction between crossing bands, a more meaningful description of the deformation pattern in this band was achieved through calculations of the spin-adiabatic type. Both calculations are discussed and compared with the experimental results. [S0556-2813(97)02202-4]

PACS number(s): 21.10.Tg, 21.10.Re, 23.20.Lv, 27.70.+q

I. INTRODUCTION

In recent years there have been numerous studies of the light W-Re-Os-Ir-Pt nuclei and most of these investigations involving the odd-Z species have led to assignments of rotational sequences built on a $1/2^+[660]$ proton configuration (e.g., see Refs. [1–7]). In most of these nuclei, the gain of alignment in this band expected from an aligning pair of $i_{13/2}$ neutrons occurs very slowly and over a large frequency range. In this region it is only for ^{171}Re that there has been observed [5] a distinct backbend in the $\pi i_{13/2}$ band, behavior which is presumed to result from a weak interaction between the ground and s bands. Recent studies [8] of ^{175}Re and ^{177}Ir have revealed upbending behavior in the $i_{13/2}$ band for both of these nuclei. In the majority of these nuclei, however, the $h_{9/2}$ band is observed and it demonstrates quite clearly a backbending behavior due to alignment of $i_{13/2}$ neutrons.

The puzzling behavior in these $\pi i_{13/2}$ bands has led to several possible explanations—no one of which can be advanced unambiguously—to account for the experimental observations. As a first consideration of this problem, let us examine the positions of the $i_{13/2}$ and $h_{9/2}$ orbitals in this region. Both are steeply downsloping intruder orbitals and, thus, are predicted [3,9,10] to be capable of driving the nucleus to larger prolate deformation. However, for most of these light odd-Z nuclei the band head built on the $1/2^-[541]$ proton configuration lies near or just below the Fermi surface, while that built on the $1/2^+[660]$ configuration lies somewhat higher above the Fermi surface. Consequently, the position of the $h_{9/2}$ orbital gives it part hole, part particle character, leaving it with very little effectiveness in driving the deformation, while the $\pi i_{13/2}$ orbital is expected to assert a strong polarization effect (e.g., see Ref. [11]).

As a consequence of this expected large deformation in these $\pi i_{13/2}$ bands, it is frequently invoked that the apparent slow alignment gain is an artifact resulting from the use of an improper reference subtraction. This is not an unreasonable assertion since with the difficulty in obtaining a good reference it is common to use for the $\pi i_{13/2}$ bands, the same reference parameters found easily for the less-deformed $h_{9/2}$ band. Although there are sound arguments for doing this, there are potential problems with such an approach as was illustrated in the recent experiments by Müller *et al.* [10] They carried out lifetime measurements in the $\pi h_{9/2}$ and $\pi i_{13/2}$ bands of ^{179}Ir and confirmed that there was significantly (and approximately constant) enhanced prolate deformation for the $i_{13/2}$ band compared with the $h_{9/2}$ band.

In their studies of ^{171}Re, Carlsson *et al.* [5] have suggested the possibility (as has been postulated [12,13] for the $5/2^+[402]$ band in ^{173}Re) that in some cases a coexistence picture may apply to the $i_{13/2}$ bands in this region, where with increasing rotational frequencies a stretching effect produces a significant shape change. One mechanism suggested [1,14,15] to account for a stretching of the nucleus in the β

*Present address: University of Liverpool, Oliver Lodge Laboratory, Liverpool, L69 3BX, England.

direction involves a large-deformation intruder band containing a $J=0$ pair of protons occupying the $1/2^-[541]$ orbital. In this picture, a three-band mixing between the $\pi i_{13/2}$ band, the $J=0$ band, and an aligned $\nu i_{13/2}$ two-quasiparticle band is carried out.

In an effort to explain the slow alignment gain in the $1/2^+[660]$ band in such nuclei as ^{175}Ir, it has been proposed [3,16] that in standard total Routhian surface (TRS) calculations there is the possibility that a strong proton-neutron (pn) interaction may not be accounted for properly. The suggested [3] remedy is to consider a residual pn interaction which is large enough to deliver a strong mixing of the one- and three-quasiparticle bands and, hence, account for smooth increases of the aligned angular momentum and the moment of inertia.

Addressing some of the common problems encountered in the nuclei in this region, Bark *et al.* [17] have carried out theoretical calculations for the light odd-even Re and Ir isotopes with $N=96$, 98, 100, and 102. They used the modified harmonic oscillator potential to calculate the properties of the diabatic [18], i.e., noninteracting, $\pi i_{13/2}$ and $\pi h_{9/2}$ g and s bands. For the one-quasiparticle $i_{13/2}$ band in most of the investigated nuclei, they found a significant shape stretching, followed by a reduction in deformation at the crossing with the s band. For the $h_{9/2}$ g and s bands, the ε_2 deformation remained nearly constant and similar to that of the bandhead deformation of the $i_{13/2}$ band. The calculations gave a satisfactory qualitative explanation of the experimental data available at the time.

The calculations of Bark *et al.* [17] also predicted that a well-defined backbending or upbending should appear in the $\pi i_{13/2}$ bands of the $N=100$ isotones, which are expected to have a weak interaction between the g and s bands. In the $N=98$ isotones, however, the interaction is expected to be larger, an effect which could obscure any upbend associated with the g-band, s-band crossing in the $i_{13/2}$ bands. Indeed, the existing data [1,2] on the $i_{13/2}$ band in ^{173}Re showed only a slow alignment gain over a wide frequency range, with no indication that it has emerged from a region of increasing alignment. At the smaller deformation of the $h_{9/2}$ band, the interaction is smaller and an upbend is expected, in accordance with the data. Subsequent experiments by Bark *et al.* [8] have verified that well-defined upbends do appear in the $\pi i_{13/2}$ band of both ^{175}Re and ^{177}Ir.

Central to a better understanding of the underlying factors that give rise to the behavior of these odd-proton nuclei discussed above is a determination of their dynamic electromagnetic transition moments which sense the collective aspects of the nuclear wave functions. In this paper we report on such measurements in ^{173}Re($Z=75$) carried out by Doppler-shift techniques. In earlier papers [12,13] we reported on lifetime measurements for states in ^{173}Re to moderately high spins by the recoil-distance method, where results for the $d_{5/2}$ band were emphasized. To gain information on states to very high spins (and resulting subpicosecond lifetimes) in the $i_{13/2}$ band of ^{173}Re, we recently carried out additional measurements on this nucleus by the Doppler-broadened line shape (DBLS) technique through the use of the GAMMASPHERE array in an early-implementational mode. These results will form the main theme of this paper.

II. EXPERIMENTAL DETAILS

To form ^{173}Re, we utilized the reaction ^{150}Sm(^{27}Al,4n)^{173}Re produced by a beam of 132-MeV ^{27}Al from the Lawrence Berkeley National Laboratory 88-inch cyclotron. Two targets were used in the experiments. One consisted of 1 mg/cm^2 ^{150}Sm evaporated onto a 42 mg/cm^2 lead backing for the DBLS measurements. The second was a 2-mg/cm^2 self-supporting ^{150}Sm evaporated foil for spectroscopy measurements. The samarium target material was enriched to 99.7% in mass 150.

Gamma-gamma coincidence measurements were carried out with the GAMMASPHERE array in an ''early-implementation'' arrangement. This consisted of five Ge detectors, each, at angles of 17.3°, 31.7°, 37.4°, 142.6°, 148.3°, and 162.7° and two detectors at 90°, with all detectors located 25.8 cm from the target. ''On-line'' gain matching of the Ge detectors was done with a ^{60}Co source, while energy and efficiency calibrations were determined from sources of ^{182}Ta and ^{152}Eu measured in both the singles and coincidence modes.

In order to avoid any potential problems from overheating of the Pb-backed ^{150}Sm target used in the DBLS experiments, the ^{27}Al beam current was limited to about 2 pnA. At this current, the γ-γ coincidence rate was 9500/sec and the γ-γ-γ rate, 2500/sec. Since, at these rates, the system dead time was only a few percent, we elected to store events of two- and higher-fold data. As the total reaction cross section was fractionated into several channels, it became necessary in the post experiment analyses of the ^{173}Re data to build γ-γ coincidence matrices from all of these stored events. Thus some degree of selectivity for the desired reaction channel was sacrificed at the expense of better statistical quality in the twofold coincidence spectra.

To further improve the quality of the data analyses, we carried out off-line gain matching of the spectra from all 32 detectors. For the analysis of the Doppler-broadened line shapes, two $5K\times5K$ coincidence matrices were constructed. One of these was from a coincidence between a γ ray detected in any one of the 15-Ge detectors in the forward three rings and an event detected in any other detector. The second matrix was composed similarly of a coincidence between any one of the backward 15 detectors and any other detector. The unsymmetrized γ-γ coincidence matrix involving the ''forward'' 15 detectors contained a total of 8.66×10^8 events, while the ''backward'' matrix contained a total of 9.00×10^8 events. As will be discussed later, it was possible to determine lifetimes independently from both the forward- and backward-shifted line shapes.

For the thin self-supporting ^{150}Sm target, it was possible to increase the ^{27}Al beam current to about 3 pnA. The accumulation of the data was carried out under essentially the same conditions as for the Pb-backed target. A basic difference in building the $5K\times5K$ coincidence matrix was that here a coincidence between any two or more detectors (regardless of angle) was considered an acceptable event. The coincidence matrix from these data contained a total of 1.02×10^9 γ-γ events. In the analysis of these coincidence data, we have only concentrated on the transitions in the $i_{13/2}$ band shown in Fig. 1 since it is necessary to know the in-band transition intensities for a determination of the inten-

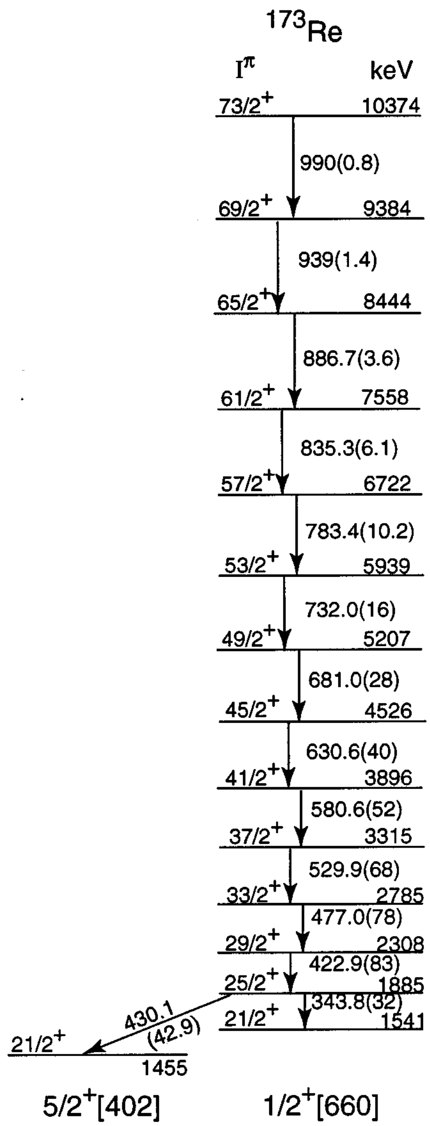

FIG. 1. Partial level scheme of ^{173}Re showing only the features relevant to the current lifetime measurements in the $i_{13/2}$ band. This band was previously assigned [1,2] as that built on the $1/2^+[660]$ proton configuration and the level scheme was developed [2] up through $I=61/2$. The three topmost levels shown here are reported for the first time in the present work. All transition energies and intensities shown are, likewise, from the current measurements. The excitation energies shown for the levels in the $i_{13/2}$ band are based on the present transition energies and the earlier energy assignment [2] of 1455 keV to a $21/2^+$ state in the $5/2^+[402]$ band. The numbers in parentheses are relative transition intensities from the present thin-target measurements.

sity of the side feeding from the continuum to each state considered. The side feeding to each state being measured is a required input parameter in our computer program for the determination of lifetimes from DBLS data.

III. ANALYSES AND RESULTS

The analyses of ^{173}Re DBLS data were carried out with the aid of the computer program LINESHAPE [19] which was originally based on a program obtained from Gascon [20,21] at the Niels Bohr Institute. The program utilizes Monte Carlo techniques, as initially applied by Bacelar *et al.* [22,23], to simulate the velocity and directional history of a series of recoiling nuclei. With the Monte Carlo routine it is possible to trace both the scattering directions and the velocities of the recoiling ions to account primarily for the nuclear stopping power where large-angle scattering and large energy losses occur. The tabulations of Northcliffe and Schilling [24] with shell corrections were used for the electronic stopping powers. For a given γ-ray transition energy, the components of the velocity distributions seen by each of the six five-detector rings were projected out and stored in ''shape vs time'' matrices containing 200 time steps over the range during which the nucleus comes to rest in the lead backing. Each matrix, with its 200 time steps by 250 channels, provides a complete set of line shapes ranging from the fully shifted ($t=0$) to the ''stopped'' peaks.

After an examination of the spectra in coincidence with each transition in the $i_{13/2}$ band and with the 430-keV interband transition to the $d_{5/2}$ band (sec Fig. 1), it was decided that the best line shape analysis would be derived from a spectrum generated by summing gates on the 430-, 423-, 477-, and 530-keV transitions. This was the case for both the forward and backward matrices. Based on the statistical quality of these γ-γ coincidence data for each five-detector angle, we elected to carry out the analyses on the sum of the 15 forward-angle detectors and on the sum of the 15 backward detectors. In the final Monte Carlo simulations for the forward-shifted and backward-shifted line shapes, equal weighting was applied to each ring of detectors.

As already mentioned, the data from the thin-target experiment have been analyzed in order to extract the relative intensities of the transitions shown in Fig. 1. Having done this, we were able to deduce for each level under consideration, the side-feeding intensity of transitions from the γ-ray continuum or from undetected discrete transitions. The line shape analysis program requires the side-feeding intensities as fixed parameters and, in addition, requires a model to handle them. We chose a side-feeding model which consists of a five-state rotational band with a fixed moment of inertia of $65\hbar^2$ MeV^{-1} and a transition quadrupole moment which can be varied during the fitting process.

The lifetime program LINESHAPE [19] carries out a χ^2 minimization of the fit for (1) Q_t, the transition quadrupole moment for the transition of interest; (2) Q_t(SF), the transition quadrupole moment for a modeled side-feeding transition; (3) a normalizing factor to normalize the intensity of the fitted transition at each angle; (4) the intercept and slope of a linear background; and (5) the intensities of contaminant peaks near the peak of interest. In our current version of the program the uncertainties in the lifetimes are determined by a statistical method using the subroutine MINOS [25]. In this procedure, it is assumed that the point in the parameter space where χ^2 takes on its lowest value $\chi^2_{\rm min}$ determines the most likely or best-fit parameter values, and that the region over which χ^2 takes on values smaller than $\chi^2_{\rm min}+1$ corresponds to the ''one-standard-deviation'' or confidence interval of 68%. The uncertainty for a given parameter was found by varying that parameter in steps above (below) its best value. At each step, this parameter was fixed and χ^2 was reminimized by varying all the other parameters. The step at which the reminimized χ^2 equaled $x^2_{\rm min}+1$ was used for the positive

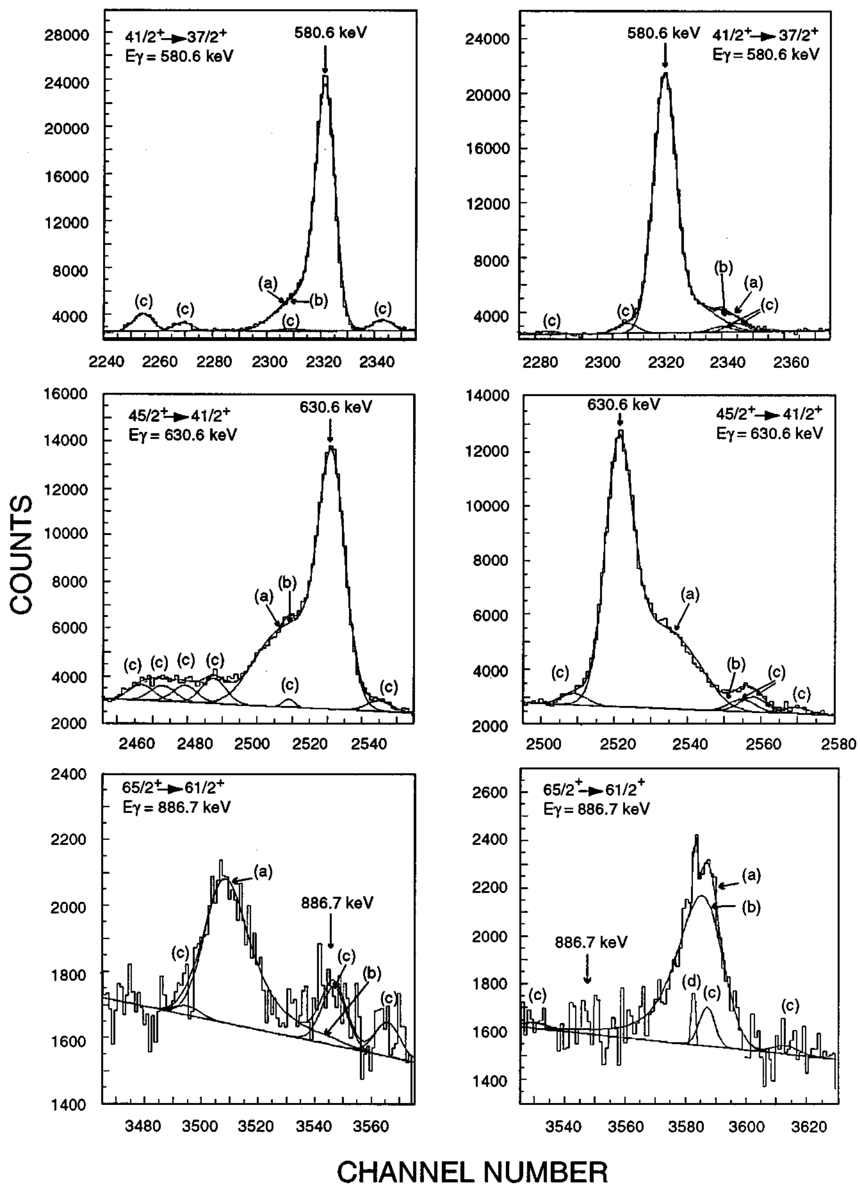

FIG. 2. Least squares fits for line shape distributions of some of the ^{173}Re γ-ray transitions in the $i_{13/2}$ band: the 580.6-keV, $41/2^+ \rightarrow 37/2^+$ transition (top two frames); the 630.6-keV, $45/2^+ \rightarrow 41/2^+$ transition (middle two frames); and the 886.7-keV, $65/2^+ \rightarrow 61/2^+$ transition (botton two frames). The left-hand frames show the data for the 15 backward detectors, and the right-hand frames show the data for the 15 forward detectors. In each frame, curve (a) is the fit to the line shape plus total background and curve (b) is the line shape fit for the transition. The peaks labeled (c) are perturbing contributions from other γ rays in the region of the line shape of interest. In the bottom right frame, the very narrow peak labeled (d) is assumed to arise from some unknown artifact introduced in the construction of the coincidence matrix.

(negative) uncertainty for this parameter. This procedure often leads to rather asymmetric error limits on some of the lifetimes and transition quadrupole moments.

For illustrative purposes, we show in Fig. 2 the least-squares fits to the line shape distributions for three of the transitions in the $1/2^+[660]$ band of ^{173}Re. These are the 580.6-keV, $41/2^+ \rightarrow 37/2^+$ transition (top two frames), the 630.6-keV, $45/2^+ \rightarrow 41/2^+$ transition (middle two frames), and the 886.7-keV, $65/2^+ \rightarrow 61/2^+$ transition (bottom two frames). For each transition, the left-hand frame shows the data for the 15 backward detectors and the right-hand frame shows the data for the 15 forward detectors. The curves labeled (a) are fits to the line shape plus total background and those labeled (b) are the line shape fits for the transition. The peaks labeled (c) are perturbing contributions from other γ rays in the region of the line shape of interest. In the bottom frames, the very narrow peak labeled (d) is presumably from some unknown artifact introduced in the construction of the coincidence matrix.

Once the decay curves had been fitted and the lifetimes and transition probabilities $[T(E2)]$ determined, it was a simple matter to extract reduced electric quadrupole transition probabilities $[B(E2)]$ and transition quadrupole moments (Q_t) by utilizing the equations

$$T(E2) = 1.23\times 10^{13} E_\gamma{}^5 B(E2), \tag{1}$$

$$B(E2;I\rightarrow I-2) = \frac{5}{16\pi}\langle I\ 2\ 0\ 0|I-2\ 0\rangle^2 Q_t{}^2, \tag{2}$$

where E_γ is in MeV, $B(E2)$ is in units of $(e\,\mathrm{b})^2$, Q_t is in $(e\,\mathrm{b})$, and the term in brackets is a Clebsch-Gordan coefficient. In the case of modeled side-feeding rotational sequences, the γ-ray energies were determined by the expression

$$E_\gamma(\mathrm{SF}) = \frac{\hbar^2(4I-2)}{2\mathscr{I}_{\mathrm{SF}}}, \tag{3}$$

where, as already pointed out, the moment of inertia for each side-feeding band $\mathscr{I}_{\mathrm{SF}}$, was assumed to be $65\hbar^2$ MeV^{-1}, which is close to that observed between low-lying members

TABLE I. Summary of results for transition quadrupole moments (Q_t) and lifetimes (τ) for high-spin states in the $1/2^+[660]$ band of ^{173}Re.

$I_i \rightarrow I_f$	E_γ (keV)	Q_t [a] (e b) (Forward-shifted data)	Q_t [b] (e b) (Backward-shifted data)	Q_t [c] (e b) Avg.	τ (ps) Avg.	Q_t(SF) [a, d] (e b) (Forward-shifted data)	Q_t(SF) [b, d] (e b) (Backward-shifted data)	Q_t(SF) [e] (e b) Avg.	τ(SF) (ps) Avg.
$41/2^+ \rightarrow 37/2^+$	580.6	$8.74^{+0.72}_{-0.58}$	$8.39^{+0.26}_{-0.23}$	$8.56^{+0.72}_{-0.58}$	$0.47^{+0.08}_{-0.06}$	$6.25^{+0.47}_{-0.47}$	$7.84^{+0.23}_{-0.10}$	$7.04^{+0.56}_{-0.56}$ [f]	$0.69^{+0.09}_{-0.09}$
$45/2^+ \rightarrow 41/2^+$	630.6	$8.20^{+0.27}_{-0.25}$	$8.04^{+0.79}_{-0.15}$	$8.12^{+0.79}_{-0.15}$	$0.34^{+0.07}_{-0.01}$	$6.23^{+0.18}_{-0.20}$	$6.19^{+0.31}_{-0.29}$	$6.20^{+0.50}_{-0.47}$ [f]	$0.58^{+0.09}_{-0.09}$
$49/2^+ \rightarrow 45/2^+$	681.0	$7.47^{+0.05}_{-0.06}$	$7.58^{+0.20}_{-0.10}$	$7.52^{+0.60}_{-0.30}$ [f]	$0.27^{+0.04}_{-0.02}$	$8.29^{+0.07}_{-0.05}$	$8.75^{+0.08}_{-0.07}$	$8.52^{+0.68}_{-0.60}$ [f]	$0.21^{+0.03}_{-0.03}$
$53/2^+ \rightarrow 49/2^+$	732.0	$8.54^{+0.89}_{-0.72}$	$7.81^{+0.32}_{-0.36}$	$8.18^{+0.89}_{-0.72}$	$0.16^{+0.03}_{-0.03}$	$6.28^{+0.32}_{-0.10}$	$7.25^{+0.27}_{-0.09}$	$6.76^{+0.54}_{-0.17}$ [f]	$0.23^{+0.04}_{-0.01}$
$57/2^+ \rightarrow 53/2^+$	783.4	$7.71^{+0.26}_{-0.22}$	$8.28^{+0.11}_{-0.93}$	$8.00^{+0.11}_{-0.93}$	$0.12^{+0.01}_{-0.03}$	$9.08^{+0.27}_{-0.24}$	$6.21^{+0.22}_{-0.22}$ [g]	$7.64^{+0.61}_{-0.54}$ [f]	$0.13^{+0.02}_{-0.02}$
$61/2^+ \rightarrow 57/2^+$	835.3	$7.84^{+0.67}_{-0.33}$	$8.00^{+0.51}_{-0.31}$	$7.92^{+0.67}_{-0.33}$	$0.088^{+0.015}_{-0.007}$	$4.02^{+0.05}_{-0.03}$	$11.9^{+0.81}_{-0.81}$ [g]	$7.96^{+0.64}_{-0.38}$ [f]	$0.087^{+0.014}_{-0.008}$
$65/2^+ \rightarrow 61/2^+$	886.7	$7.67^{+0.78}_{-0.49}$	$8.51^{+1.31}_{-0.74}$	$8.09^{+1.31}_{-0.74}$	$0.062^{+0.020}_{-0.011}$	$7.42^{+0.65}_{-0.35}$	$6.22^{+0.66}_{-0.66}$ [g]	$6.82^{+0.65}_{-0.35}$	$0.088^{+0.017}_{-0.009}$
$69/2^+ \rightarrow 65/2^+$	939.4	$8.14^{+1.33}_{-0.94}$	$8.02^{+1.32}_{-1.01}$	$8.08^{+1.32}_{-1.01}$	$0.047^{+0.015}_{-0.011}$	$6.98^{+0.38}_{-0.36}$	$5.86^{+0.21}_{-0.19}$	$6.27^{+0.50}_{-0.48}$ [f]	$0.078^{+0.012}_{-0.012}$

[a]Arithmetic average of several fits to the experimental data for the forward-shifted line shapes. The error shown is the largest value from any MINOS fit used in obtaining the average Q_t value.

[b]Arithmetic average of several fits to the experimental data for the backward-shifted line shapes. The error shown is the largest value from any MINOS fit used in obtaining the average Q_t value.

[c]Arithmetic average of the Q_t values shown in columns 3 and 4. The error limit is the larger of that in columns 3 and 4, with the exception noted in footnote f.

[d]Q_t (SF) is the effective quadrupole transition moment for a modeled side-feeding cascade consisting of five rotational states having a moment of inertia of 65 $\mathrm{MeV}^{-1}\hbar^2$.

[e]Arithmetic average of the values shown in columns 7 and 8. The error limit is the larger of that in columns 7 and 8, with the exception noted in footnote f.

[f]The minimum acceptable final error limit has been set subjectively at 8%. The largest MINOS error limit from any fit used in obtaining this average Q_t value has been adjusted upward to conform to this criterion.

[g]Gaussian error fit—unable to obtain a satisfactory MINOS fit.

of the $i_{13/2}$ band and was held constant in the fitting process. Varying this value by as much as 5% in the model caused negligible changes in the $E2$ transition rates between members of the $i_{13/2}$ band.

In earlier spectroscopy studies of ^{173}Re, transitions in the $i_{13/2}$ band were assigned [2] up through a spin of $61/2^+$. However, from our thin-target data we find three new transitions in this band, extending the levels up to $I=73/2$. From the DBLS results, we have determined lifetimes and the associated Q_t values of two of these new levels labeled with $I=65/2$ and 69/2 ($E_\gamma=886.7$ and 939.4 keV, respectively), along with the next six lower levels, down to $I=41/2^+$.

A summary of the results from the current measurements is presented in Table I. Numerous fits were carried out on both the forward- and backward-shifted data where we employed variations in the fitting parameters and the numbers of levels grouped in a given fit. Average values of Q_t were then taken for each transition in the two sets (forward and backward shifted) of data. Columns 3 and 4 of Table I show these average values derived from the forward- and backward-shifted line shapes, respectively. For each transition, the error limit shown is the largest value obtained with the MINOS procedure in any fit used in the averaging. In column 5 we show for each transition the ''accepted'' Q_t value, which is just the arithmetic average of the values in columns 3 and 4. The error on the accepted value is the larger of the two MINOS values used in the averaging except for the cases noted in the table. Similarly, the corresponding average values of Q_t(SF), the effective quadrupole transition moments for the modeled side-feeding rotational cascades, are shown in columns [7–9]. Although done in a subjective manner (but based on our past experiences with such data), we set 8% as the minimum acceptable error limit for the larger of the positive or the negative MINOS error on the final average in-band and side-feeding quadrupole transition moments. The cases where error limits were increased to this value are so noted in Table I. The lifetimes corresponding to the accepted Q_t values are listed in column 6, and the associated effective side-feeding lifetimes, τ_t(SF), are listed in column 10.

IV. DISCUSSION

The final average values of the transition quadrupole moments (Q_t) for transitions in the $i_{13/2}$ band of ^{173}Re (from column 5 of Table I) are shown as solid circles in Fig. 3. Within the error limits, it is possible to fit all of the $E2$ transitions from states with $I=41/2$–$69/2$ (corresponding to a frequency range of $\hbar\omega=0.29$–0.47 MeV) by a constant value of $Q_t=8.1\pm0.5$ e b, which corresponds to $\beta_2\approx0.29$. Because of the longer lifetimes of lower states in the band, it was not possible to obtain information on them in these DBLS experiments. However, we do have lifetime information on the $29/2^+ \rightarrow 25/2^+$, 422.9-keV transition from our earlier recoil-distance measurements [12,26]. The Q_t value extracted for this transition in those data is 8.2 ± 1.3 e b, and

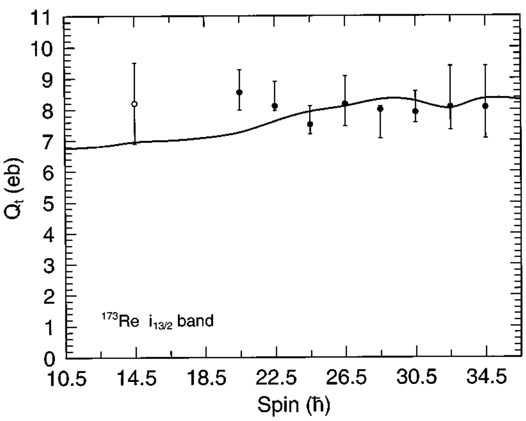

FIG. 3. Transition quadrupole moments (Q_t) for the $\pi i_{13/2}$ band in ^{173}Re. The solid circles are from the present DBLS measurements. As explained in the text, the error limits shown are in each case the largest MINOS error from any fit used in obtaining the final average Q_t value plotted here. The open circle, for the spin-29/2 state, is from earlier recoil-distance measurements [26]. The solid curve represents Q_t values calculated from the wave functions of a spin-adiabatic configuration.

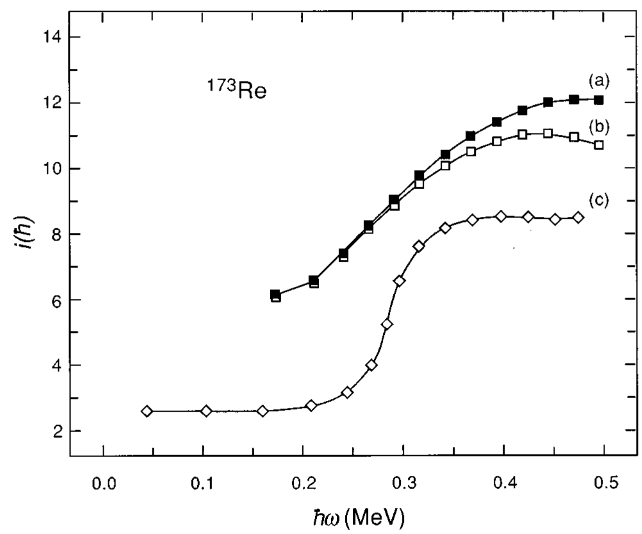

FIG. 4. Experimental alignments for the $\pi i_{13/2}$ and $\pi h_{9/2}$ bands in ^{173}Re. Curve (a) is considered a good fit to the experimental data for the $i_{13/2}$ band where the moments of inertia reference parameters $\mathscr{I}_0 = 32.2\hbar^2$ MeV^{-1} and $\mathscr{I}_1 = 65.6\hbar^4$ MeV^{-3} were used in the reference subtraction. Curve (b) is the fit obtained for the $i_{13/2}$ band with the parameters $\mathscr{I}_0 = 31.6\hbar^2$ MeV^{-1} and $\mathscr{I}_1 = 79.4\hbar^4$ MeV^{-3}, which are the values determined from a fit for the $h_{9/2}$ band shown in curve (c).

it is shown as an open circle in Fig. 3. Therefore, we are left with a picture that is compatible with a rather large and near-constant deformation in the $i_{13/2}$ band, but which, because of the large error limits, could be accommodated by a relatively small stretching at lower frequencies ($\hbar\omega < 0.29$ MeV).

As a first step in exploring the conclusions that may be drawn from the data in Fig. 3, we consider the matter of alignment gain in the $i_{13/2}$ bands of ^{173}Re and some of its neighbors. In order to extract an aligned angular momentum which can be interpreted in a meaningful way, a reference configuration with well-understood properties must be chosen. For most cases in the vicinity of ^{173}Re, this has been a rather difficult task. Except for ^{171}Re, which shows a backbend in the $\pi i_{13/2}$ band [5], and for ^{175}Re and ^{177}Ir, which show upbends in this band [8], it has not been possible from experimental data to assign reliable alignment gains and band-crossing frequencies to the presumed alignment of $i_{13/2}$ neutrons in these nuclei.

In the Introduction we alluded to the general problems faced with the gradual gain in angular momentum in the rotational bands built on the 1/2[660] configuration in this region, as compared to the $h_{9/2}$ rotational bands. The possible explanations for this behavior include a large and constant deformation, a gradually increasing deformation, and an extraordinarily large interaction between the g and s bands. From the work of Bark *et al.* [17], one concludes that for most of these nuclei, use of the $i_{13/2}$ one-quasiparticle band itself as a reference should probably be avoided. A better reference is usually provided by the $h_{9/2}$ one-quasiparticle bands which are believed to have a nearly constant deformation and a g-band, s-band interaction that is well understood [17]. Furthermore, deformations calculated [17] for diabatic configurations in nuclei in this region are such that the same reference is expected to be relevant near the bandhead of the one-quasiparticle $i_{13/2}$ band and for the s bands built on both the $i_{13/2}$ and $h_{9/2}$ configurations. This means that the alignment extracted for these bands should directly reflect the contribution from the excited quasiparticles. It is only for the higher-spin members of the $i_{13/2}$ one-quasiparticle band that a significant contribution originating from a difference in deformation should be expected.

The analysis performed in Ref. [17] showed that a common reference (viz., $\mathscr{I}_0 = 30\hbar^2$ MeV^{-1} and $\mathscr{I}_1 = 77\hbar^4$ Mev^{-3}) could be used for several Ir and Re isotopes near $N = 100$ and that, with only modest variations from nucleus to nucleus, the $h_{9/2}$ s bands have an aligned angular momentum of about $9\hbar$. To this total alignment, the odd proton is assumed to contribute about $3\hbar$ and the aligned pair of neutrons about $6\hbar$. Further, they [17] observed that the $i_{13/2}$ s bands have aligned angular momenta of about $13\hbar$, shared nearly equally between the odd proton and the aligned pair of $i_{13/2}$ neutrons.

In light of the above discussion, let us now examine plots of aligned angular momentum vs. rotational frequency for the $\pi i_{13/2}$ and $\pi h_{9/2}$ bands in ^{173}Re. These are shown in Fig. 4. After we [27] incorporated two additional levels at the top of the $h_{9/2}$ band based on current measurements, it was found that the alignment in this band is described only moderately well by the common reference parameters used in Ref. [17] for this region. However, we find that a better fit is given by $\mathscr{I}_0 = 31.6\hbar^2$ Mev^{-1} and $\mathscr{I}_1 = 79.4\hbar^4$ Mev^{-3} as used in curve (c) of Fig. 4 where a total alignment of $8.5\hbar$ is achieved. About $2.5\hbar$ of this alignment can be attributed to the odd proton and about $6\hbar$ to the aligned pair of $i_{13/2}$ neutrons. When those same reference parameters are used for the $i_{13/2}$ band, the results in curve (b) are obtained. The problem here is that while about $6.2\hbar$ of alignment is reasonable for the odd $i_{13/2}$ proton, the indicated gain of about $4.9\hbar$ from alignment of a pair of $i_{13/2}$ neutrons is less than expected. Curve (a) is a plot of the $i_{13/2}$ band with the use of reference parameters $\mathscr{T}_0 = 32.2\hbar^2$ MeV^{-1} and $\mathscr{T}_1 = 65.6\hbar^4$ MeV^{-3}. This seems a more plausible description of this band as, here about $6.1\hbar$ of alignment is carried by the odd proton and an additional $6\hbar$ is gained in the alignment of $i_{13/2}$ neutrons. When compared with the reference parameters for the $h_{9/2}$ band, this increase in $\mathscr{T}_0$ and reduction in $\mathscr{T}_1$ are not conclusive evidence of, but are consistent with, an increased deformation and increased rigidity, respectively, in the $i_{13/2}$ band. Note that the three new transitions we have assigned to the top of the $i_{13/2}$ band have enabled us to determine that the initial phase of alignment has completed at $\hbar\omega \sim 0.45$ MeV since the region of the expected strong interaction between the crossing bands appears to have disappeared at frequencies higher than this.

Overall, the experimental alignments determined for the $h_{9/2}$ and $i_{13/2}$ bands of ^{173}Re in the present measurements are reasonably well accounted for (at least qualitatively) by the deformations from the diabatic calculations [17]. However, the actual deformations that come out of the diabatic treatment for the $i_{13/2}$ band of ^{173}Re do not fit well with our experimental results. The calculations [17] showed a large shape stretching up to the crossing with the *s* band, followed by a significant reduction in deformation above the crossing frequency. An examination of the Q_t values in Fig. 3 shows that this is hardly the case. We note, however, that in the case of ^{179}Ir such a reduction in Q_t values is observed in experimental data [10] for states with spins of 45/2 and 49/2 where the *s* band mixes into the yrast band.

The interaction between the $i_{13/2}$ *g* and *s* bands in ^{173}Re depends strongly on the deformation of the nucleus; viz., the interaction strength increases with increasing deformation. At deformations corresponding to those determined in the current measurements for the upper part of the *g* band, the interaction is calculated to be about 350 keV. Consequently, the above discussed treatment of diabatic bands with no interaction cannot provide a fully satisfactory description of the $i_{13/2}$ band. A calculation of the type carried out in Ref. [18] where spin-adiabatic configurations were employed is probably a better alternative, as in this approach a strong interaction between the *g* and *s* bands is retained, contrary to the situation for a pure diabatic treatment. In the spin-adiabatic treatment it is only the weakly interacting bands that are replaced by sharply crossing diabatic bands. Therefore, we have performed spin-adiabatic calculations for ^{173}Re, following exactly the prescriptions given in Ref. [18].

In the spin-adiabatic calculations we observe a shape stretching for the lower part of the $i_{13/2}$ *g* band, in close agreement to what was calculated [17] for the diabatic $i_{13/2}$ *g* band. However, in the band-crossing region (spins roughly between 20 and 30), the spin-adiabatic calculations are tracing the yrast line, which at large deformations is pushed down considerably due to the very large interaction between the *g* and *s* bands. At smaller deformations, representative of the diabatic $i_{13/2}$ *s* band ($\beta_2 \approx 0.25$), the *g*-band, *s*-band interaction is much smaller and, in fact, is removed in the calculations (cf. Fig. 3 in Ref. [18]), resulting in no suppression at all of the yrast line (cf. Fig. 2 in Ref. [18]). This changes the energy balance between large deformation ($\beta_2 \approx 0.30$) and small deformation ($\beta_2 \approx 0.25$) in favor of the larger deformations. Although the energy surfaces are soft in the band-crossing region, the energy minimum for the yrast $i_{13/2}$ band remains at a large deformation throughout the band-interaction region and even above spin 30. (The same effect has been observed in TRS calculations in which band interactions are not removed.)

Allowing for the uncertainties pointed out above, a direct comparison between the experimental data and the theoretical Q_t values, calculated from the wave functions of the spin-adiabatic configuration, is made in Fig. 3 (solid curve). The agreement is good for spins above $20\hbar$. A proper treatment of the theoretical interaction between the ground and *s* bands (which is not a straightforward matter) is, however, expected to reduce the Q_t values for the highest points to values which probably would fall below the error bars. Below spin 20 only one experimental point is known [26], namely, for spin 29/2. This point lies high above the calculated value, but the error bar is large and overlaps the theoretical curve. The theoretical Q_t values are, therefore, hardly inconsistent with the experimental data, but the data are equally consistent with a large and constant Q_t value. The same is true for the data for ^{179}Ir [10]. In order to finally determine whether the deformation of the $i_{13/2}$ *g* band is constant or increasing with spin, high-quality recoil-distance data are required.

In conclusion, we shall summarize several important points relative to the current measurements on ^{173}Re and to the general features of the $i_{13/2}$ bands in neighboring nuclei.

(1) The current measurements indicate that a large and near-constant deformation ($\beta_2 \approx 0.29$) characterizes the $i_{13/2}$ band of ^{173}Re over the frequency range of 0.29–0.47 MeV.

(2) The Q_t values found here for the $i_{13/2}$ band of ^{173}Re are considerably larger than those for the $h_{9/2}$ band [27]. This feature is consistent with the pattern for this region of nuclei where the $h_{9/2}$ orbital lies below the Fermi surface while the $i_{13/2}$ orbital lies above, but near, the Fermi surface.

(3) When compared with the current experiment, the results of both the diabatic and the spin-adiabatic calculations for the $i_{13/2}$ band show points of agreement. However, there are also enough disagreements with experiment in these calculations to leave us without a fully consistent explanation of the behavior of the $i_{13/2}$ band. The diabatic calculations give a reasonable accounting of the gain in aligned angular momentum, but they do not take into consideration the strong interaction between the ground and *s* bands. Further, in the diabatic approach the experimentally aligned angular momentum demands a reduced deformation in the *s* band, contrary to what is seen. The spin-adiabatic calculations, however, show quite good agreement with the experimental Q_t values for the *s* band, but predict for the *g* band a reduced deformation which is barely overlapping with the error bars for the single experimentally measured value [26] at $I = 29/2$. Unfortunately, this leaves us unable to make a definitive statement of whether the ground band has a constant or a gradually increasing deformation.

(4) No distinct upbending is observed in ^{173}Re, in contrast to the $N = 100$ isotones ^{175}Re and ^{177}Ir, but this was hardly expected, due to the large *g*-band, *s*-band interaction at $N = 98$. On the other hand, the alignment saturates for the highest spins, which are supposedly belonging to the *s* band,

at a value similar to those observed in the $N=100$ isotones as predicted in Ref. [17].

(5) We are unable to determine if a large proton-neutron interaction is a contributor to the pattern of slow alignment gain in the $i_{13/2}$ band of ^{173}Re. However, the upbends in ^{175}Re and ^{177}Ir and the backbending in ^{171}Re rule out the possibility that a large *p-n* interaction can be the general explanation for the behavior of these $i_{13/2}$ bands.

(6) There is considerable need for additional lifetime measurements on $i_{13/2}$ bands of nuclei in this region. In particular, high-quality recoil-distance measurements on members of the $i_{13/2}$ *g* band of ^{173}Re are needed, and both recoil-distance and DBLS measurements are important for ^{177}Ir and ^{175}Re, which show upbending in their $i_{13/2}$ bands.

ACKNOWLEDGMENTS

The authors would like to express their appreciation to all of the members of the GAMMASPHERE project and to the members of the LBL 88 inch-Cyclotron staff for their help during the course of these measurements. We are also grateful for discussions with R. Wyss. This research was sponsored by the U.S. Department of Energy, under Contract No. DE-AC05-96OR22464 with Lockheed Martin Energy Research Corporation. The Joint Institute for Heavy Ion Research has as member institutions the University of Tennessee, Vanderbilt University, and the Oak Ridge National Laboratory; it is supported by the members and by the U.S. Department of Energy through Contract No. DE-FG05-87ER40361 with the University of Tennessee.

[1] R. A. Bark, G. D. Dracoulis, A. E. Stuchbery, A. P. Byrne, A. M. Baxter, F. Riess, and P. K. Weng, Nucl. Phys. **A501**, 157 (1989).
[2] L. Hildingsson, W. Klamra, Th. Lindblad, G. G. Linden, C. A. Kalfas, S. Kossionides, C. T. Papadopoulos, R. Vlastou, J. Gizon, D. Clarke, F. Khazaie, and J. N. Mo, Nucl. Phys. **A513**, 394 (1990).
[3] B. Cederwall, B. Fant, R. Wyss, A. Johnson, J. Nyberg, J. Simpson, A. M. Bruce, and J. N. Mo, Phys. Rev. C **43**, 2031 (1991).
[4] S. Juutinen, P. Ahonen, J. Hattula, R. Julin, A. Pakkanen, A. Virtanen, J. Simpson, R. Chapman, D. Clarke, F. Khazaie, J. Lisle, and J. N. Mo, Nucl. Phys. **A526**, 346 (1991).
[5] H. Carlsson, M. Bergström, A. Brockstedt, L. P. Ekström, J. Lyttkens-Linde´n, H. Ryde, R. A. Bark, G. B. Hagemann, J. D. Garrett, R. Chapman, D. Clarke, F. Khazaie, J. C. Lisle, and J. N. Mo, Nucl. Phys. **A551**, 295 (1993).
[6] H.-Q. Jin, L. L. Riedinger, C. R. Bingham, M. P. Carpenter, V. P. Janzen, C.-H. Yu, L. Zhou, P. B. Semmes, J.-Y. Zhang, M. A. Riley, C. Baktash, M. L. Halbert, N. R. Johnson, I.-Y. Lee, and F. K. McGowan, Phys. Rev. C **53**, 2106 (1996).
[7] H.-Q. Jin, L. L. Riedinger, C.-H. Yu, W. Nazarewicz, R. Wyss, J.-Y. Zhang, C. Baktash, J. D. Garrett, N. R. Johnson, I. Y. Lee, and F. K. McGowan, Phys. Lett. B **277**, 387 (1992).
[8] R. A. Bark, S. W. Odegård, R. Bengtsson, I. G. Bearden, G. B. Hagemann, B. Herskind, F. Ingebretsen, S. Leoni, H. Ryde, T. Shizuma, K. Strähle, P. O. Tjǿm, and J. Wrzesinski, Phys. Rev. C **52**, R450 (1995).
[9] W. Nazarewicz, M. A. Riley, and J. D. Garrett, Nucl. Phys. **A512**, 61 (1990).
[10] D. Müller, A. Virtanen, R. Julin, S. Juutinen, A. Lampinen, M. Piparinen, S. Törmänen, F. Christiancho, A. P. Byrne, G. D. Dracoulis, B. Fabricius, C. Fahlander, A. Johnson, K. P. Lieb, J. Nyberg, I. Thorslund, and R. Wyss, Phys. Lett. B **332**, 265 (1994).
[11] L. L. Riedinger, in *Progress in Particle and Nuclear Physics*, edited by A. Faessler (Pergamon Press, Oxford, 1992), Vol. 28, p. 75.
[12] N. R. Johnson, in *Nuclear Physics of Our Times*, edited by A. V. Ramayya (World Scientific, Singapore, 1993), p. 149.
[13] N. R. Johnson, J. C. Wells, F. K. McGowan, D. F. Winchell, I.-Y. Lee, R. Wyss, W. C. Ma, W. B. Gao, C.-H. Yu, and S. Pilotte, Nucl. Phys. **A557**, 347 (1993).
[14] G. D. Dracoulis, R. A. Bark, A. E. Stuchbery, A. P. Byrne, A. M. Baxter, and F. Riess, Nucl. Phys. **A486**, 414 (1988).
[15] R. A. Bark, J. Phys. G **17**, 1209 (1991).
[16] R. Wyss and A. Johnson, in *Proceedings of the International Conference on High Spin Physics and Gamma-Soft Nuclei*, edited by J. X. Saladin, R. A. Sorensen, and C. M. Vincent (World Scientific, Singapore, 1991), p. 123.
[17] R. A. Bark, R. Bengtsson, and H. Carlsson, Phys. Lett. B **339**, 11 (1994).
[18] R. Bengtsson, T. Bengtsson, M. Bergström, H. Ryde, and G. B. Hagemann, Nucl. Phys. **A569**, 469 (1994).
[19] J. C. Wells and N. R. Johnson, ''LINESHAPE: A Computer Program for Doppler-Broadened Lineshape Analysis,'' Report No. ORNL-6689 (1991), p. 44.
[20] J. Gascon (private communication).
[21] J. Gascon, C.-H. Yu, G. B. Hagemann, M. P. Carpenter, J. M. Espino, Y. Iwata, T. Komatsurbara, J. Nyberg, S. Ogaza, G. Sletten, P. O. Tjǿm, D. C. Radford, J. Simpson, A. Alderson, M. A. Bentley, P. Fallon, P. D. Forsyth, J. W. Roberts, and J. F. Sharpey-Schafer, Nucl. Phys. **A513**, 344 (1990).
[22] J. C. Bacelar (private communication).
[23] J. C. Bacelar, A. Holm, R. M. Diamond, E. M. Beck, M. A. Deleplanque, J. Draper, B. Herskind, and F. S. Stephens, Phys. Rev. Lett. **57**, 3019 (1986); Phys. Rev. C **35**, 1170 (1987).
[24] L. C. Northcliffe and R. F. Schilling, Nucl. Data Tables **7**, 233 (1970).
[25] F. James and M. Roos, Comput. Phys. Commun. **10**, 343 (1975).
[26] N. R. Johnson, J. C. Wells, F. K. McGowan, D. F. Winchell, I.-Y. Lee, R. Wyss, W. C. Ma, W. B. Gao, C.-H. Yu, and S. Pilotte (unpublished).
[27] J. C. Wells, N. R. Johnson, C. J. Gross, C. Baktash, D. M. Cullen, Y. Akovali, F. K. McGowan, M. J. Brinkman, H.-Q. Jin, W. T. Milner, C.-H. Yu, I.-Y. Lee, and A. O. Macchiavelli (unpublished).